ADVANCED
FUNCTIONAL
MATERIALS

Supporting Information

for *Adv. Funct. Mater.*, DOI 10.1002/adfm.202405291

Radiation Hardness and Defects Activity in PEA_2PbBr_4 Single Crystals

Andrea Ciavatti, Vito Foderà, Giovanni Armaroli, Lorenzo Maserati, Elisabetta Colantoni, Beatrice Fraboni and Daniela Cavalcoli*

Supporting Information

Radiation Hardness and Defects Activity in PEA_2PbBr_4 Single Crystals

Andrea Ciavatti[1], Vito Foderà[1], Giovanni Armaroli[1], Lorenzo Maserati[1], Elisabetta Colantoni[1], Beatrice Fraboni[1], Daniela Cavalcoli[1]*

[1]Department of Physics and Astronomy – Alma Mater Studiorum University of Bologna, Viale Berti-Pichat 6/2, 40127 Bologna, Italy

*Corresponding Author

Email: andrea.ciavatti2@unibo.it

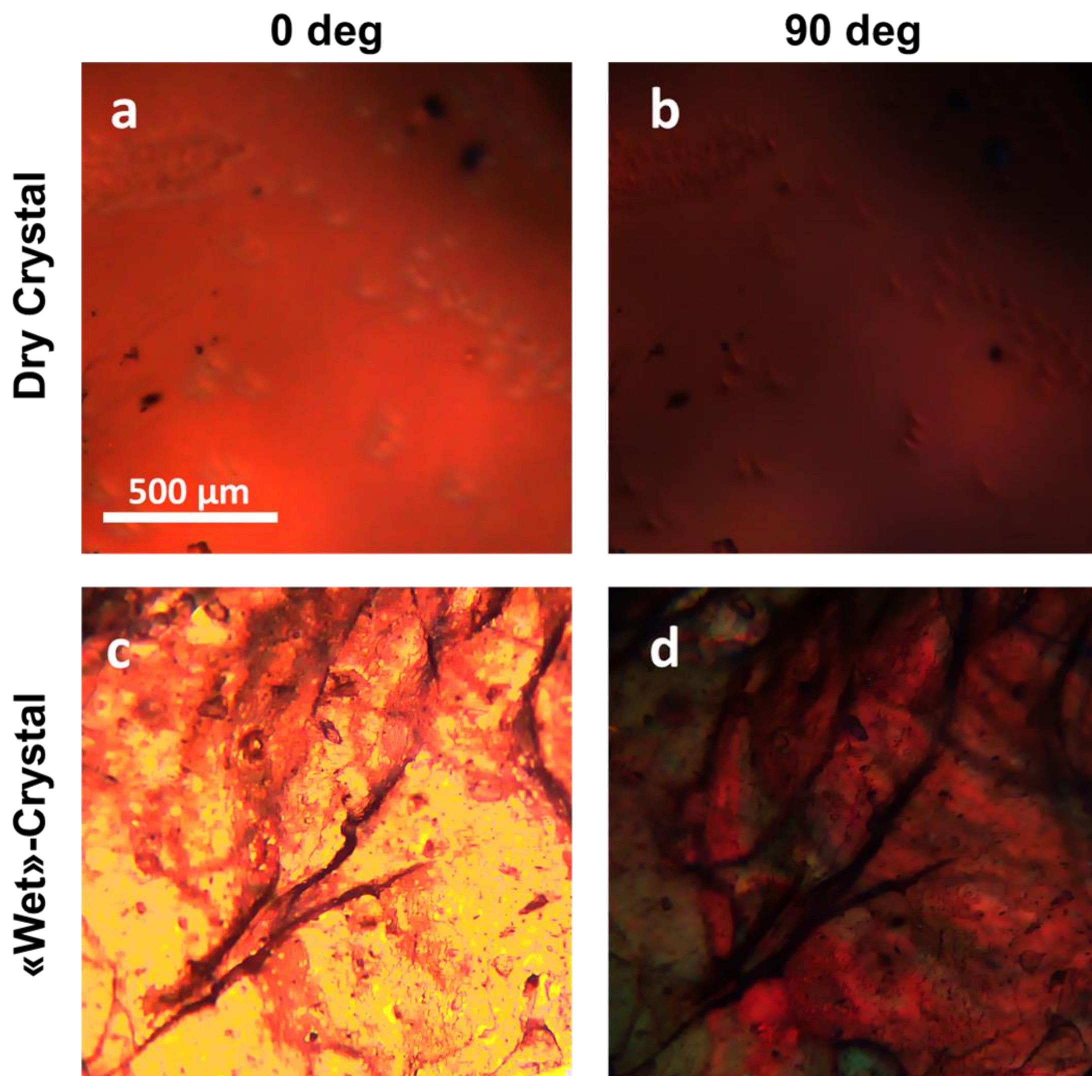

Figure SI 1. Optical microscopy images under polarized light of the surface of *dry* crystal (*sample 2* – a, b) and *wet* crystal (*sample 3* – c, d).

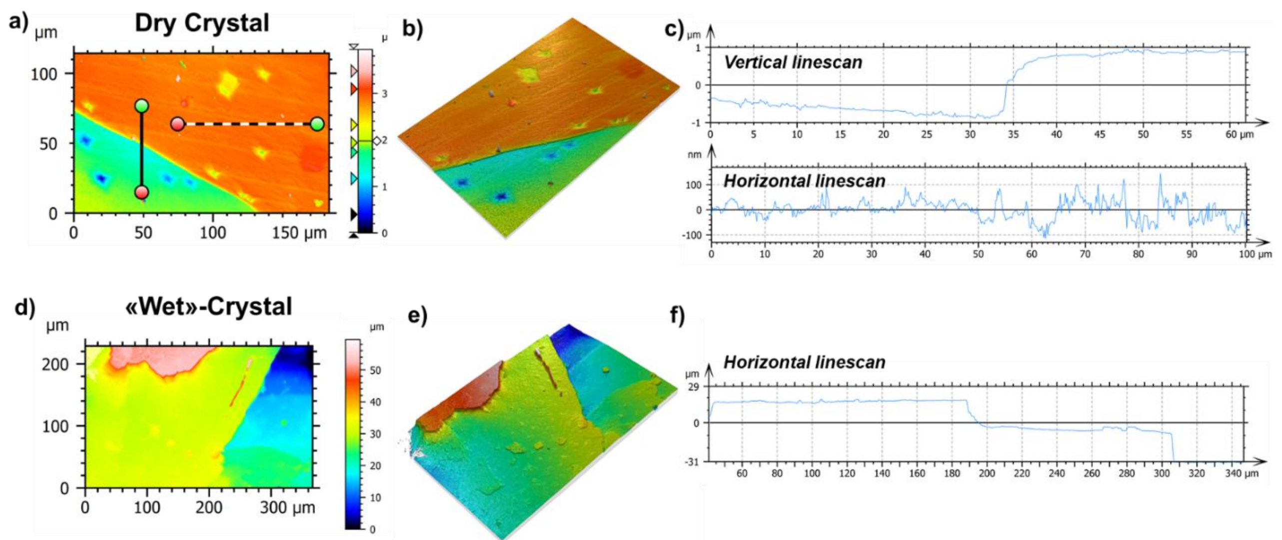

Figure SI 2. Optical WLI interferometer images and profiles. Surface colormap (a), 3D map representation (b), vertical and horizontal linescans (c) of *dry* crystal. Surface colormap (d), 3D map representation (e), horizontal linescan (f) of *wet* crystal.

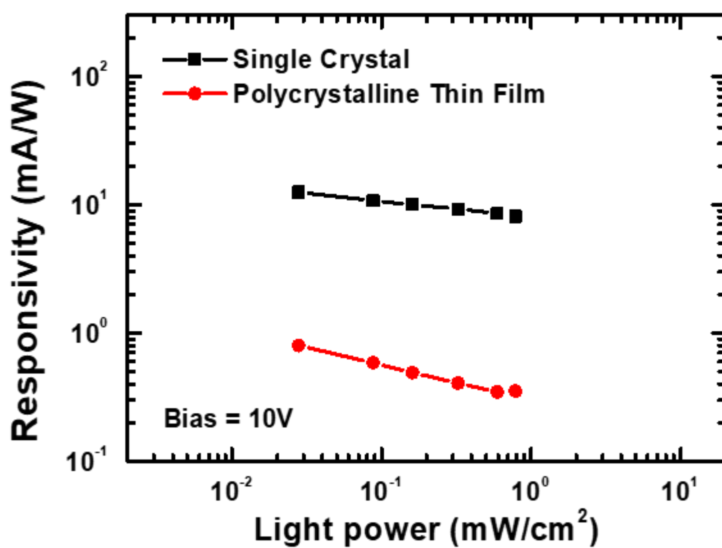

Figure SI 3. Responsivity comparison between free-standing single crystal and spin-coated polycrystalline film.

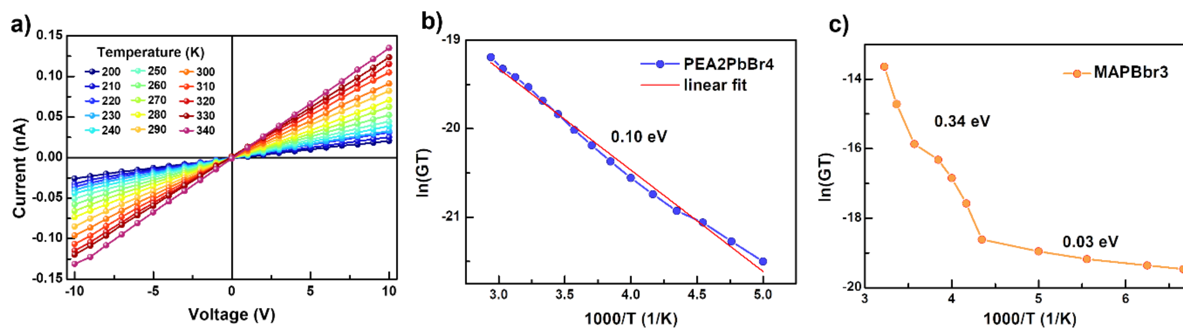

Figure SI 4: Temperature dependence of electrical conductivity**.** a) Current-Voltage characteristics in dark and under vacuum in the temperature range spanning from 200 K to 340 K. 10K step between each plot. b,c) Logarithm of electrical conductivity vs. *1/T* showing the linear behaviour of Nernst-Einstein equation for 2D perovskite PEA_2PbBr_4 (b) and 3D perovskite $MAPbBr_3$ (c).

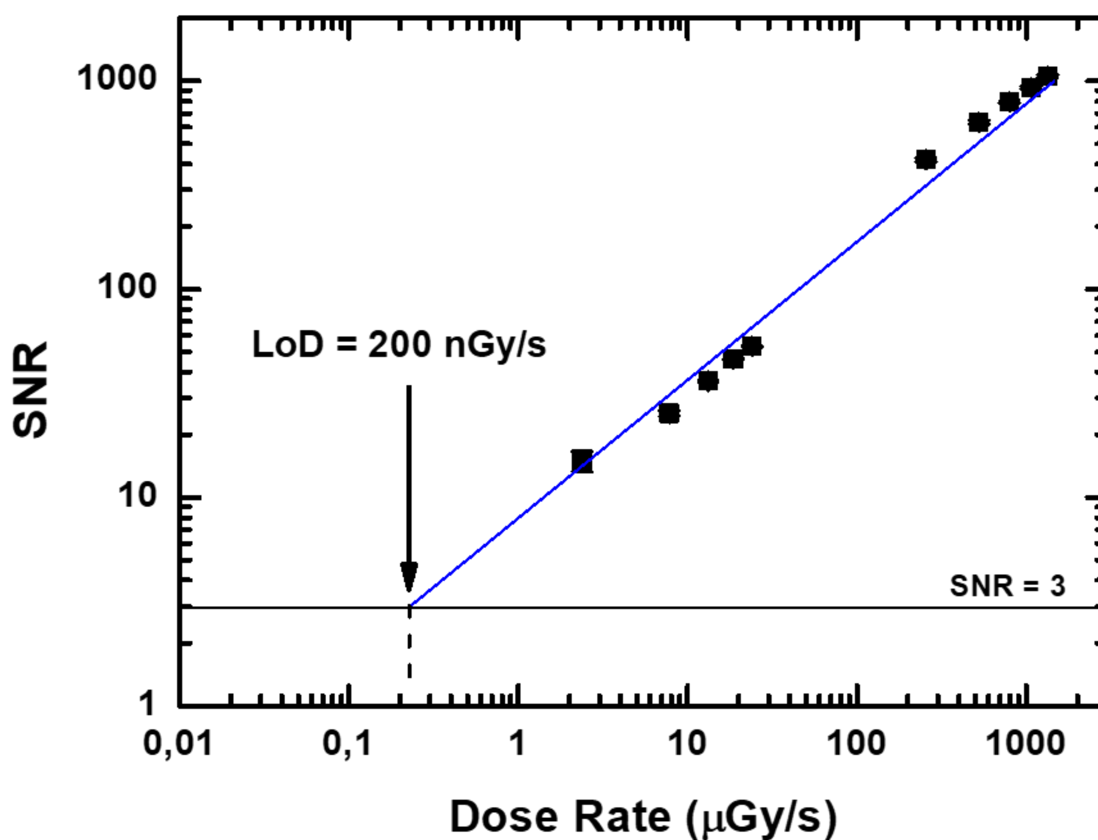

Figure SI 5. Signal-to-noise Ratio (SNR) at low dose rates to calculate the Limit of Detection (LoD) under X-ray irradiation. Bias of 10V.

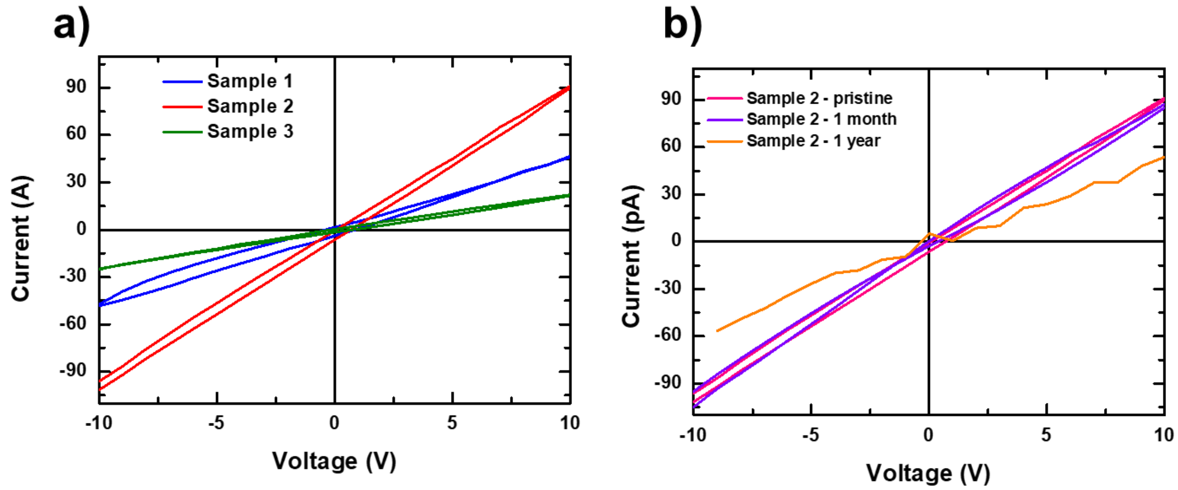

Figure SI 6. A) I-V graph of all the three samples showing the ohmic behaviour. b) the I-V plot of *sample 2* showing no changing of dark current after 1 month, and small degradation after 1 year.

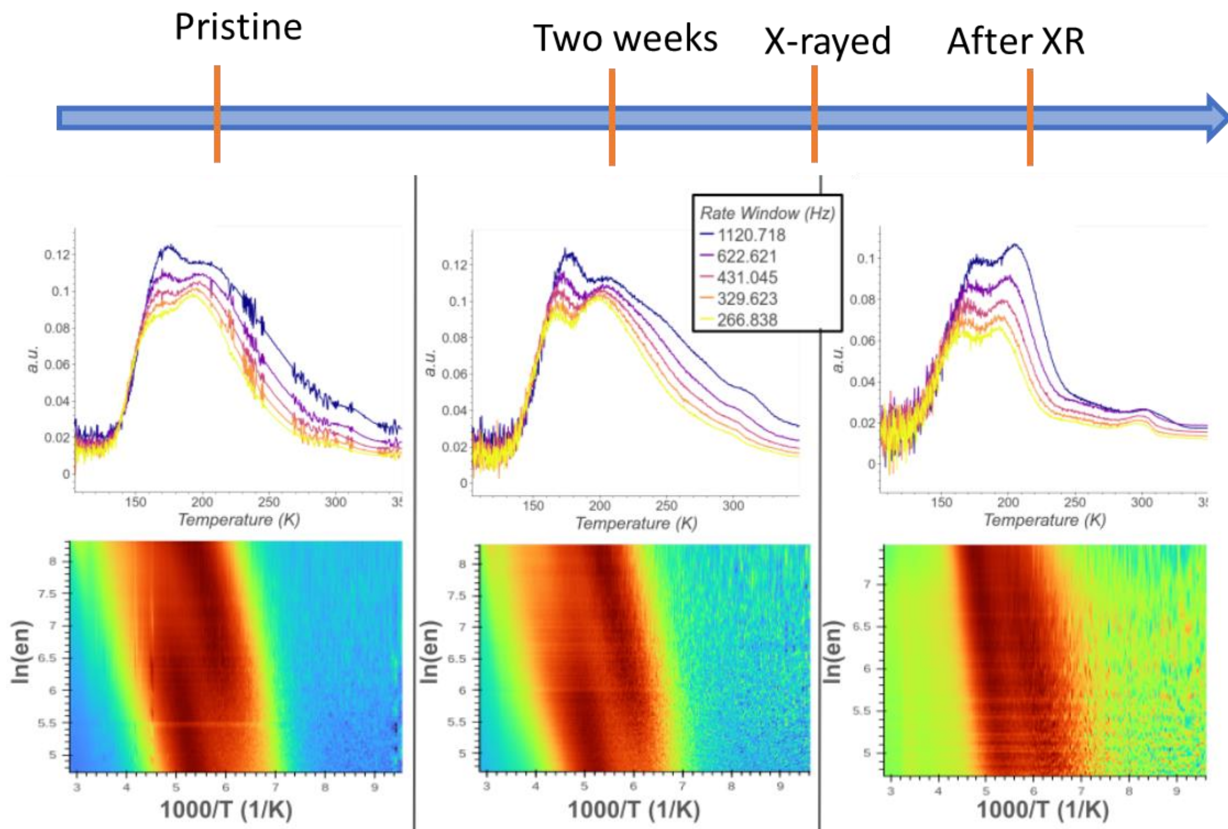

***Figure SI 7**. PICTS spectra and color maps of* sample 1*: pristine, 2 weeks old and after X-ray irradiation .*

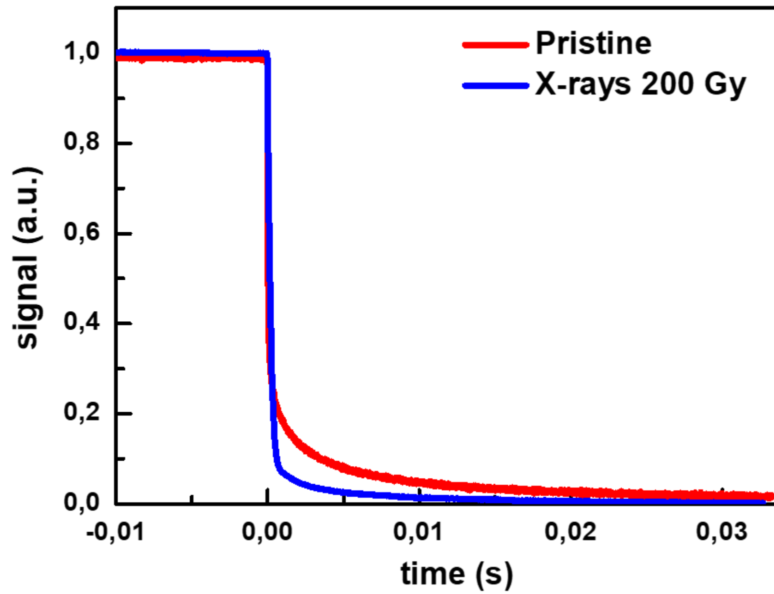

Figure SI 8. Collection of current transients as the temperature changes, compared before X-ray exposure and after X-ray exposure.

	Resistance (Ω)	**ΔI (nA) @10V**	**Responsivity (mA/W)**	**D* (Jones)**
		As-grown		
Sample 2 – dry	$(1.5 \pm 0.2) \times 10^{11}$	2.44	2.3×10^{-2}	3.2×10^{8}
Sample 3 - wet	$(1.7 \pm 0.3) \times 10^{13}$	15.9	15×10^{-2}	5.1×10^{10}
		2 years		
Sample 2 – dry	$(6.6 \pm 0.1) \times 10^{11}$	3.05	2.9×10^{-2}	1.1×10^{9}
Sample 3 - wet	$(1.2 \pm 0.1) \times 10^{13}$	0.22	0.2×10^{-2}	2.4×10^{7}

Table SI 1. Optoelectronic properties of *sample 2* and *sample 3* as-grown and after 2 years.

Technical Note 1

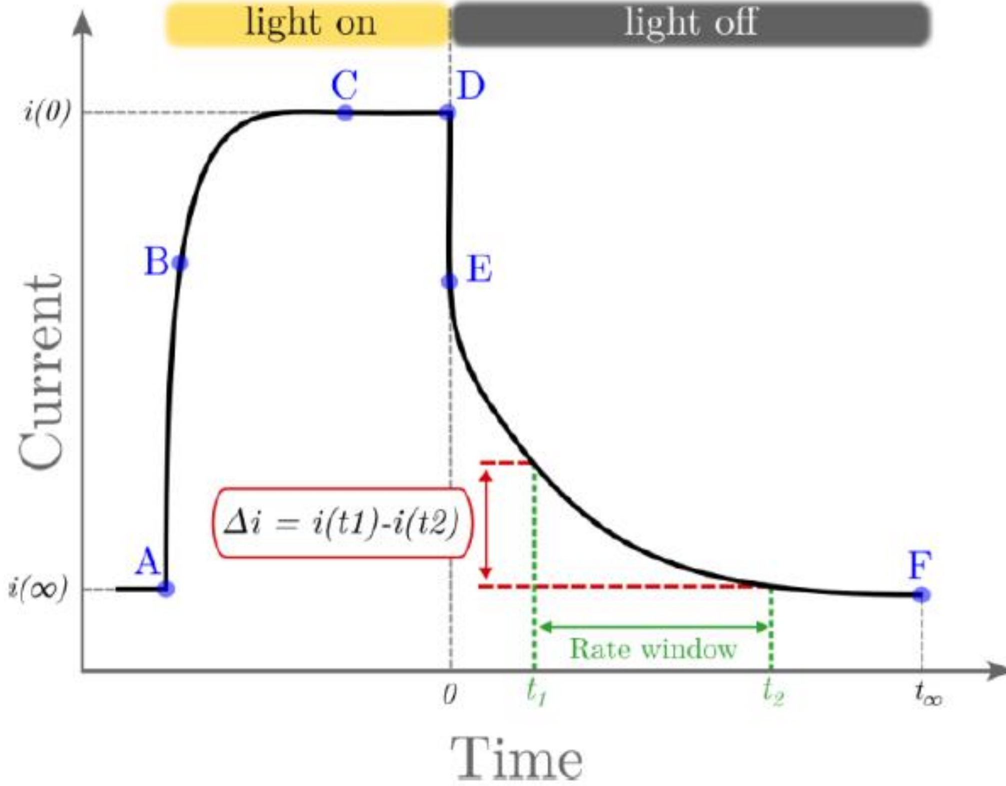

Figure SI 9. Schematic representation of the double-gate rate window method on an ideal photocurrent transient. Points A, B, C, D and E represent the key points in time where different phenomena take place, as described in the text.

As expressed by Equation (1) the emission rate from a single trap state has an exponential behaviour with the temperature. The relevant trap parameters that can be extracted by PICTS are the activation energy of the defect Ea and its capture cross section σ. Expressing the temperature dependence of vn and Nc allows to formulate the expression that is key for defect level characterization, as it defines the so-called *Arrhenius plot*.

$$\ln\left(\frac{T^2}{e_t}\right) = \gamma\sigma + \frac{E_a}{kT} \tag{1}$$

where γ contains universal constants and the effective mass of the semiconductor under study.
In this work we analysed the photocurrent decay transients with the method called "rate window" method, which is a numerical one, that does not rely on fitting. The method is based on the work of Balland et al. [1,2]
We make use of the double-gate method, schematized in **Figure SI 9**. It consists of choosing two-time instants t_1 and t_2, called *gates*, that define a rate window of duration t_2-t_1. The PICTS signal for such rate window is defined as the difference between current at time t_1 and time t_2, calculated as a function of temperature $\Delta i(T)=i(t_1, T)-i(t_2, T)$ (see Equation 2). It can be shown that the $\Delta i(T)$ shows a maximum at temperature Tm, which, through Equation (1), corresponds to a specific

emission rate $e_t(T_m)$. The condition for the maximum can be found by maximizing the $\Delta i(T)$ function, which yields:

$$e_t(t_2 - t_1) = \ln\left(\frac{e_t\, t_2 - 1}{e_t\, t_1 - 1}\right) \tag{2}$$

where e_t is calculated at temperature T_m. The last Equation is key for relating theory (through e_t) and experiment (through t_1 and t_2). Indeed, once the rate window is chosen by setting t_1 and t_2, the corresponding emission rate is fixed by this equation. This is a transcendental equation and can be solved numerically to find e_t.

The theory reported above assumes that the mobility μ_n and lifetime τ_n of carriers are temperature-independent. This is often not the case, and such dependence may introduce artefacts in the spectra. To overcome this issue, we normalised all the transients by the photocurrent value, i.e. $i_{norm}(t) = \frac{i(t) - i_\infty}{i_0 - i_\infty}$. This procedure removes from i(t) the dependence from $\mu\tau$ product. Then, the double-gate analysis as described above can be applied to $i_{norm}(t)$. In this work, all PICTS spectra were obtained with the normalized double-gate method, since all samples showed a temperature dependence of the mobility-lifetime product.

Technical Note 2

The broadening of the peaks in transient spectroscopy methods is generally associated to a distribution of multiple trap activation energies, due to disorder in the material. This effect has been described by Das et al. (Semicond. Sci. Technol. 3 (1988) 1177-1183). Briefly, they discriminate between “weak disorder” where the correction to activation energies are negligible; and “strong disorder” where the activation energies extracted by the Arrhenius plot are overestimated. The parameter σ/E_0 is used to separate the weak disorder ($\sigma/E_0 \leq 0.1$) from strong disorder ($\sigma/E_0 > 0.1$). It is possible to evaluate the disorder regime of each peak by considering the phenomenological relationship connecting the FWHM (ΔT), the peak temperature (T_m) and σ, by Murawala et al. [Phys. Rev.B, 1984, 29, 4807].:

$$\Delta T / T_m = 0.1 + \sigma / E_0 \tag{3}$$

Below the fraction evaluated for T1, T2 and T3.

	T_m	ΔT – FWHM	σ/E_0
T1	~ 156 K	24 K	0.05
T2	~ 190 K	58 K	0.21
T3	~ 309 K	57 K	0.08

Table SI 2. Temperature of the peak maximum (T_m), FWHM of the peak (ΔT) and the corresponding σ/E_0 as calculated by the Muralawa relationship.

Technical Note 3

Commonly used Hecht formula foresees localized charge density generation close to one of the electrodes [3]. Thus, low penetrating radiations (UV-VIS light or α-particles) are used to fulfil the requirements in vertical sandwich-like detectors. However, the charge collection in detectors with absorption-limited sensitivity [4] and with uniform absorption through the volume (e.g. thin detectors, highly penetrating γ rays) [5,6] has been studied. The volumes are sliced into thin layers assuming uniform carrier's generation in each layer. Then, the collection efficiency $\eta(x)$ from every slice could be calculated using the position dependent Hecht formula [6]:

$$\eta(x) = \frac{N_{coll}\,(x)}{N_{gen}} = s_h/d\left(1 - e^{-\frac{d-x}{s_h}}\right) + s_e/d\left(1 - e^{-\frac{x}{s_e}}\right) \tag{4}$$

Where,

x is the distance from the anode to the charge generation position;

$N_{coll}(x)$ are the collected charges at position x;

N_{gen} is the total generated charges;

d is the distance between electrodes;

$s_{h,e} = \frac{\mu_{h,e}\tau_{h,e}V}{d}$ is the *schubweg*;

The total collected charges above uniform carrier generation could be found by integrating the above expression:

$$N_{coll} = N_{gen}\, s_h/d \int_0^d \left(1 - e^{-\frac{d-x}{s_h}}\right)\frac{dx}{d} + N_{gen}\, s_e/d \int_0^d \left(1 - e^{-\frac{x}{s_e}}\right)\frac{dx}{d} \tag{5}$$

$$N_{coll} = N_{gen}\left[x_h\left(1 + x_h\left(e^{-\frac{1}{x_h}} - 1\right)\right) + x_e\left(1 + x_e\left(e^{-\frac{1}{x_e}} - 1\right)\right)\right] \tag{6}$$

Where $x_{h,e} = \frac{s_{h,e}}{d} = \frac{\mu_{h,e}\tau_{h,e}V}{d^2}$.

The case of uniform linearly generated carriers in co-planar geometry is similar to the one illustrated above, thus, considering single carrier transport the photocurrent ΔI vs voltage V is:

$$\Delta I = C \cdot N_{coll} = I_{sat}\,\frac{\mu\tau\, V}{d^2}\left(1 + \frac{\mu\tau\, V}{d^2}\left(e^{-\frac{d^2}{\mu\tau\, V}} - 1\right)\right) \tag{7}$$

Equation 7 above have been used to fit the experimental data in Figure 2c.

[1] J. C. Balland, J. P. Zielinger, C. Noguet, M. Tapiero, *J. Phys. D: Appl. Phys.* **1986**, *19*, 57.
[2] J. C. Balland, J. P. Zielinger, M. Tapiero, J. G. Gross, C. Noguet, *J. Phys. D: Appl. Phys.* **1986**, *19*, 71.
[3] K. Hecht, *Z. Physik* **1932**, *77*, 235.
[4] M. Z. Kabir, S. O. Kasap, *Appl. Phys. Lett.* **2002**, *80*, 1664.
[5] K.-O. Kim, T.-J. Kwon, J. K. Kim, J.-H. Ha, *Journal of the Korean Physical Society* **2011**, *59*, 20.
[6] O. Semeniuk, O. Grynko, G. Decrescenzo, G. Juska, K. Wang, A. Reznik, *Sci Rep* **2017**, *7*, 8659.